CM in directions perpendicular to the helical screw axis of the phase.

Conclusions

Detailed analysis of dynamic quenching data reveal that the preferred orientations for quenching pyrene singlets by a sterically hindered alkylamine, CA, in a nonpolar solvent, CM, is very specific and resembles closely the geometry (E) thought to be assumed by the corresponding exciplex.

Two separate methods for calculation of the activation parameters for pyrene singlet quenching in CM lead to very similar results: the activation energy in the cholesteric phase at low CA concentrations ($E_6 = 9.9 \pm 0.2$ and 11.8 ± 0.7 kcal mol^{-1} by the two methods) is about twice that in the isotropic phase ($E_6 = 5.3 \pm 0.1$ and 5.4 ± 1.4 kcal mol^{-1}). The entropy of activation in the cholesteric phase of CM is more positive than in the isotropic phase since the transition state is more disruptive of liquid crystalline order than are the dissociated reactants.

The magnitude of E_a(cholesteric) is *not* constant, but decreases with increasing CA concentration, approaching E_a(isotropic). The decrease is a consequence of CA disrupting the liquid crystalline order of CM, making the quenching transition state between pyrene and CA easier to attain.

Acknowledgment. We thank Dr. Dan Martire and the reviewers for their helpful suggestions. The National Science Foundation (Grant CHE-7906572) and the Naval Research Laboratory are acknowledged for their financial support of this research.

Appendix

As mentioned in the text, the method employed in calculating the activation parameters from the d(ln τ)/d($1/T$) slopes (Figure 2; column a and b of Table II) makes no assumptions concerning the reversibility of the pyrene–CA exciplex. The sole condition, that the pyrene decay times be much longer than those of the exciplex, is met. The second method employs the limiting Stern–Volmer slopes from Figure 4 with a quenching constant, $k_q = k_6$. If reverisiblity were significant, then eq 19 would hold. Substitution of Arrhenius expressions for k_6, k_7, and k_8 followed by differentiation of ln k_q yields eq 20.

$$k_q = k_6k_8/(k_7 + k_8) \tag{19}$$

$$\frac{\mathrm{d}\ln k_q}{\mathrm{d}(1/T)} = \frac{-E_6}{R} - \frac{E_8}{R} + \frac{A_7E_7e^{-E_7/RT} + A_8E_8e^{-E_8/RT}}{R(A_7e^{-E_7/RT} + A_8e^{-E_8/RT})} \tag{20}$$

If reversibility is important, the activation energies in column c of Table II are equal to $E_6 + E_8 - (A_7E_7e^{-E_7/RT} + A_8E_8e^{-E_8/RT})/(A_7e^{-E_7/RT} + A_8e^{-E_8/RT})$. Therefore, $E_8 - (A_7E_7e^{-E_7/RT} + A_8E_8e^{-E_8/RT})/(A_7e^{-E_7/RT} + A_8e^{-E_8/RT})$ can be no larger than the difference between the activation energies in column c and either a or b.

That this difference is very small (and probably zero within the limits of *accuracy*) requires that either (1) $E_7 \simeq E_8$ or (2) $A_7E_7e^{-E_7/RT} \ll A_8E_8e^{-E_8/RT}$ and $A_7e^{-E_7/RT} \ll A_8e^{-E_8/RT}$. Any other condition would predict a temperature dependent value for the difference such that the Arrhenius slopes in Figure 5 would not be linear.

In the first case, reversibility is important and $k_7 \gg k_8$ because of entropy factors. Due to decreased solvent viscosity, exciplex dissociation increases with increasing temperature more rapidly than emission or nonradiative deactivation pathways.[22] Therefore, the correspondence between the activation energies in Table II ought to be much worse in the isotropic phase of CM than in its much more viscous cholesteric phase. In fact, the activation energies are equal.

The second condition makes exciplex formation irreversible: $k_7 \ll k_8$. In this case, $R[\mathrm{d}\ln k_q/\mathrm{d}(1/T)] = E_6$ and the activation energies calculated by the two methods should be very similar, as observed.

Photochemistry of the Tetranuclear Clusters $H_2Ru_4(CO)_{13}$, $H_2FeRu_3(CO)_{13}$, and $H_2FeOs_3(CO)_{13}$[†]

Henry C. Foley and Gregory L. Geoffroy*

Contribution from the Department of Chemistry, The Pennsylvania State University, University Park, Pennsylvania 16802.

Received May 17, 1981.
Revised Manuscript Received August 10, 1981

Abstract: Photolysis of $H_2FeRu_3(CO)_{13}$, $H_2Ru_4(CO)_{13}$, and $H_2FeOs_3(CO)_{13}$ in the presence of PPh_3 and H_2 leads to formation of the corresponding $H_2M_4(CO)_{12}(PPh_3)$ and $H_4M_4(CO)_{12}$ clusters with moderate efficiency. The 366-nm quantum yields for PPh_3 substitution are 0.030, 0.016, and 0.057, respectively. Photolysis of these clusters in the presence of CO leads to cluster fragmentation but with low quantum efficiency ($\phi \leq 10^{-5}$). The quantum yield for PPh_3 substitution in $H_2FeRu_3(CO)_{13}$ is independent of PPh_3 concentration but is decreased in the presence of added CO, implying competition of CO with PPh_3 for a photogenerated intermediate. The mechanism most consistent with all the experimental observations is one involving CO dissociation in the primary photochemical event, and not metal–metal bond homolysis.

Monomeric metal carbonyl complexes generally lose carbon monoxide upon photolysis whereas the dominant photoreaction for dinuclear carbonyls, such as $Mn_2(CO)_{10}$, is rupture of the metal–metal bond.[1] The latter process is believed to arise from excited states involving net population of metal–metal antibonding orbitals, depopulation of the corresponding bonding orbitals, or both.[1] Consider next metal carbonyl clusters which contain more than one metal–metal bond. Will these undergo net photofragmentation via metal–metal bond rupture with more or less efficiency than photoinduced CO dissociation? The reported spectral data for this class of compounds certainly indicates that the lowest-lying excited states are localized predominantly within the metal–metal bonded framework,[2–6] and thus photolysis would be

---

[†] Dedicated to George S. Hammond on the occasion of his 60th birthday.

(1) Geoffroy, G. L.; Wrighton, M. S. "Organometallic Photochemistry"; Academic Press: New York, 1979.

(2) Epstein, R. A.; Gaffney, T. R.; Geoffroy, G. L.; Gladfelter, W. L.; Henderson, R. S. *J. Am. Chem. Soc.* **1979**, *101*, 3847.

0002-7863/81/1503-7176$01.25/0 © 1981 American Chemical Society

expected to result in rupture of metal–metal bonds and fragmentation of the cluster. However, the extent of metal–metal bond cleavage in a cluster framework produced by absorption of a single photon may not be sufficient to give net fragmentation, since the remaining metal–metal bonds may serve to hold the framework together. The excitation energy could then be released via CO dissociation.

Metal–metal bond cleavage does appear to dominate the photochemistry of trinuclear clusters, although truly definitive studies are lacking. Certainly $Fe_3(CO)_{12}$,[7] $Ru_3(CO)_{12}$,[8] and $H_3Re_3(CO)_{12}$[2] fragment upon photolysis, but the mechanisms by which these reactions occur have not been conclusively delineated. Conversely, $Os_3(CO)_{12}$ does not fragment upon photolysis but instead gives clean photosubstitution chemistry.[3] This may be due to the increased strength of the Os–Os bonds in the latter cluster,[9,10] thus rendering metal–metal bond rupture less efficient than CO dissociation.

Few studies of tetranuclear clusters have been reported and these have relatively little mechanistic detail. Johnson, Lewis, and co-workers[11] have shown that photolysis of $H_4Os_4(CO)_{12}$ gives clean photosubstitution chemistry; analogous results were obtained by Wrighton and co-workers[12] for $H_4Ru_4(CO)_{12}$. The tentative conclusion that may be drawn is that for clusters with nuclearity ≥ 4, photodeclusterification does not obtain and the net photochemistry involves CO loss. Whether this is because the metal–metal excited states, which clearly lie lowest in energy, are too delocalized to give cleavage of a single metal–metal bond or whether such cleavage does occur but net fragmentation is inhibited by the remaining metal–metal bonds is an unanswered question. We have undertaken a comparative, quantitative study of the photochemistry of a series of tetranuclear clusters in order to address this question and determine the relative efficiency of photoinduced fragmentation compared to CO loss. The results of our study of $H_2FeRu_3(CO)_{13}$, $H_2Ru_4(CO)_{13}$, and $H_2FeOs_3(CO)_{13}$ are reported herein. X-ray crystallographic studies have shown that the solid-state structures of $H_2FeRu_3(CO)_{13}$[13] and $H_2Ru_4(CO)_{13}$[14] are that depicted in **1** (M = Fe, Ru) and spectroscopic data imply a similar geometry for $H_2FeOs_3(CO)_{13}$.[5,15,16]

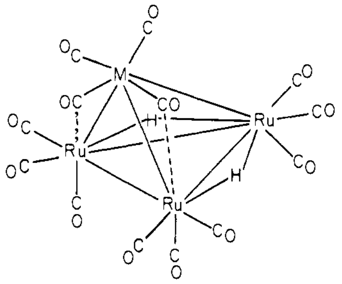

1

Table I. Electronic Absorption Spectral Data[a]

cluster	λ_{max}, nm (ϵ_{max}, $M^{-1}\ cm^{-1}$) 300 K	λ_{max}, nm (ϵ_{max}, $M^{-1}\ cm^{-1}$) 77 K
$H_2FeRu_3(CO)_{13}$	540 (1013)	530 (1417)
	381 (8040)	379 (9266)
	340 (10300)	336 (12100)
$H_2Ru_4(CO)_{13}$	556 (1079)	521 (2325)
	444 (3230)	426 (4340)
	357 (10470)	354 (19250)
$H_2FeOs_3(CO)_{13}$	468 (1202)	453 (3220)
	408 (3125)	395 (6009)
	340 (8654)	340 (10570)

[a] Cyclohexane–pentane (7:4) solution. The 77 K extinction coefficients have been corrected for 15% solvent contraction upon cooling from 300 to 77 K.

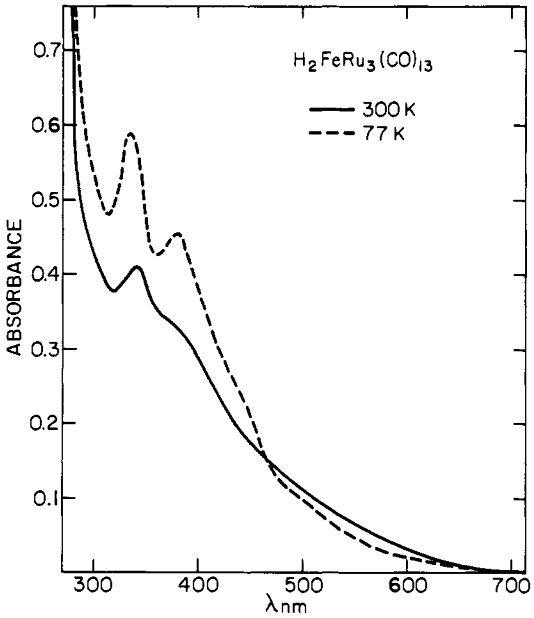

Figure 1. Electronic absorption spectra of $H_2FeRu_3(CO)_{13}$ at 300 K (—) and 77 K (---) measured in cyclohexane–pentane (7:4) solution. The 77 K spectrum is corrected for 15% solvent contraction upon cooling.

Experimental Section

The clusters $H_2FeRu_3(CO)_{13}$,[5] $H_2FeRu_3(CO)_{12}(PPh_3)$,[17] $H_2FeRu_3(CO)_{11}(PPh_3)_2$,[17] $H_2FeOs_3(CO)_{13}$,[16] and $H_2Ru_4(CO)_{13}$[18] were prepared according to published procedures. All solvents employed were dried and degassed by standard methods. Isooctane was further purified by passage over $AgNO_3$-coated alumina.

General Photochemical Procedures. Aliquots (2 to 5 mL) of solutions of each cluster, generally in isooctane, were irradiated in 25-mL Schlenk vessels fitted either with a serum cap or with Kontes quick-release Teflon valves and ground glass joints for attachment to a high-vacuum line. Where appropriate, PPh_3 was added to give solutions containing two- to fivefold excess PPh_3 over cluster. All solutions were thoroughly degassed via 4 freeze–pump–thaw cycles and the appropriate gaseous atmosphere admitted. The course of the reactions was monitored by removing aliquots with a gas-tight syringe and analyzing by IR spectroscopy or analytical liquid chromatography, using the previously described chromatography apparatus.[17] Photolyses were conducted with a Hanovia 450 W medium-pressure Hg discharge lamp, a 100 W Blak-Ray B100A lamp equipped with a 366-nm narrow band-pass filter, or on an optical bench equipped with a water-cooled lamp housing (Photochemical Research Associates, Inc., Model ALH215), a 100 W high-pressure Hg arc lamp (Osram HBO 100 w/2), a monochromator (Photochemical Research Associates, Inc., Model B102), and a water-jacketed 1-cm UV–vis spectrophotometer cell holder. Light intensities (366 nm, 4.4×10^{-7}

---

(3) Tyler, D. R.; Altobelli, M.; Gray, H. B. *J. Am. Chem. Soc.* **1980**, *102*, 3022.

(4) Geoffroy, G. L.; Epstein, R. A. *Inorg. Chem.* **1977**, *16*, 2795.

(5) Geoffroy, G. L.; Gladfelter, W. L. *J. Am. Chem. Soc.* **1977**, *99*, 7565.

(6) Tyler, D. R.; Levenson, R. A.; Gray, H. B. *J. Am. Chem. Soc.* **1978**, *100*, 7888.

(7) Austin, R. G.; Paonessa, R. S.; Giordano, P. J.; Wrighton, M. S. *Adv. Chem. Ser.* **1978**, *168*, 189.

(8) Johnson, B. F. G.; Lewis, J.; Twigg, M. V. *J. Organomet. Chem.* **1974**, *67*, C75.

(9) Connor, J. A.; Skinner, H. A.; Virnani, Y. *Symp. Faraday Soc.* **1973**, *8*, 18.

(10) Quicksall, C. Q.; Spiro, T. G. *Inorg. Chem.* **1968**, *7*, 2365.

(11) (a) Johnson, B. F. G.; Kelland, J. W.; Lewis, J.; Rehani, S. K. *J. Organomet. Chem.* **1976**, *113*, C42. (b) Bhaduri, S.; Johnson, B. F. G.; Kelland, J. W.; Lewis, J.; Raithby, P. R.; Rehani, S.; Sheldrick, G. M.; Wong, K.; McPartlin, M. *J. Chem. Soc., Dalton Trans.* **1979**, 562.

(12) Graff, J. L.; Wrighton, M. S. *J. Am. Chem. Soc.* **1980**, *102*, 2123.

(13) Gilmore, C. J.; Woodward, P. *J. Chem. Soc. A* **1971**, 3453.

(14) Yawney, D. B. W.; Doedens, R. J. *Inorg. Chem.* **1972**, *11*, 838.

(15) Moss, J. R.; Graham, W. A. G. *J. Organomet. Chem.* **1970**, *23*, C23.

(16) Burkhardt, E. W.; Geoffroy, G. L. *J. Organomet. Chem.* **1980**, *198*, 179.

(17) Fox, J. R.; Gladfelter, W. L.; Wood, T. G.; Smegal, J. A.; Foreman, T. K.; Geoffroy, G. L.; Tavaniepour, I.; Day, V. W.; Day, C. S. *Inorg. Chem.* **1981**, *20*, 3214.

(18) Knox, S. A. R.; Koepke, J. W.; Andrews, M. A.; Kaesz, H. D. *J. Am. Chem. Soc.* **1975**, *97*, 3942.

Table II. Quantum Yield Data for PPh_3 Photosubstitution[a]

cluster	[cluster], M	$[PPh_3]$, M	ϕ
$H_2FeRu_3(CO)_{13}$	3.65×10^{-4}	3.65×10^{-4}	0.025 ± 0.006
	3.65×10^{-4}	1.83×10^{-3}	0.029 ± 0.006
	3.65×10^{-4}	3.65×10^{-3}	0.030 ± 0.006
$H_2FeOs_3(CO)_{13}$	5.28×10^{-4}	2.6×10^{-3}	0.057 ± 0.012
$H_2Ru_4(CO)_{13}$	3.00×10^{-4}	1.5×10^{-3}	0.016 ± 0.002

[a] Isooctane solution.

einsteins/min) were measured by ferrioxalate actinometry.[19] Quantum yields were determined by measuring the difference in cluster concentration before and after photolysis from liquid chromatographic peak areas, relative to toluene as an internal standard. These analyses were conducted using a μ-Porasil (silica) column and hexane as the eluting solvent with a flow rate of 1.0 mL/min.

Results

Electronic Absorption Spectra. Electronic absorption spectral data for $H_2FeRu_3(CO)_{13}$, $H_2FeOs_3(CO)_{13}$, and $H_2Ru_4(CO)_{13}$ are set out in Table I and the spectra of $H_2FeRu_3(CO)_{13}$ at 300 and 77 K are shown in Figure 1. Each cluster shows a series of poorly resolved bands in the 300–600 nm region which sharpen and shift slightly in position upon cooling to 77 K. Specific assignments cannot presently be made for these bands except to note that they are probably due to transitions localized primarily within the metal framework on the basis of similar spectral assignments for the corresponding $M_3(CO)_{12}$ (M = Fe, Ru, Os) trimers.[6,20]

Photosubstitution of PPh_3 for CO. Photolysis of $H_2FeRu_3(CO)_{13}$, $H_2Ru_4(CO)_{13}$, and $H_2FeOs_3(CO)_{13}$ in hydrocarbon solution in the presence of PPh_3 gives clean photosubstitution of PPh_3 for CO, eq 1. The course of these reactions was monitored by IR spectroscopy and by high-pressure analytical liquid chromatography (LC). A typical LC chromatogram is shown in Figure 2. The $H_2FeRu_3(CO)_{13-x}(PPh_3)_x$ (x = 1, 2) derivatives were identified by comparison of their IR spectra to reported spectra[17] and by comparison of their LC retention times to those of authentic samples. ^1H, ^{31}P, and ^{13}C NMR studies, described in detail elsewhere,[17,21] have shown that $H_2FeRu_3(CO)_{12}(PPh_3)$ and $H_2FeRu_3(CO)_{11}(PPh_3)_2$ have the structures depicted in 2 and 3 with substitution occurring solely on the Ru atoms. The $H_2Ru_4(CO)_{13}$ and $H_2FeOs_3(CO)_{13}$ substituted derivatives were independently prepared in batch scale photolysis experiments and were characterized by their infrared and mass spectra.[22,23] The order of LC peak development and the IR spectral changes during photolysis clearly indicate that the monosubstituted derivatives are the primary photoproducts. The disubstituted products arise from photolysis of the monosubstituted derivatives. Products arising from fragmentation of the tetranuclear clusters were not generally observed unless the PPh_3 was present in large excess or the reactions were prolonged.[24]

$$H_2M_4(CO)_{13} + PPh_3 \xrightarrow[25\ °C,\ \text{isooctane}]{h\nu} H_2M_4(CO)_{13-x}(PPh_3)_x + xCO \qquad (1)$$

$$x = 1, 2$$

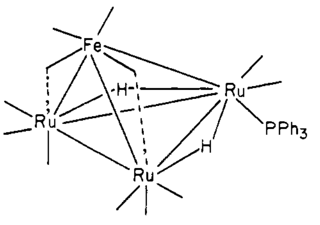

2

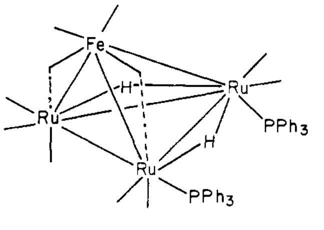

3

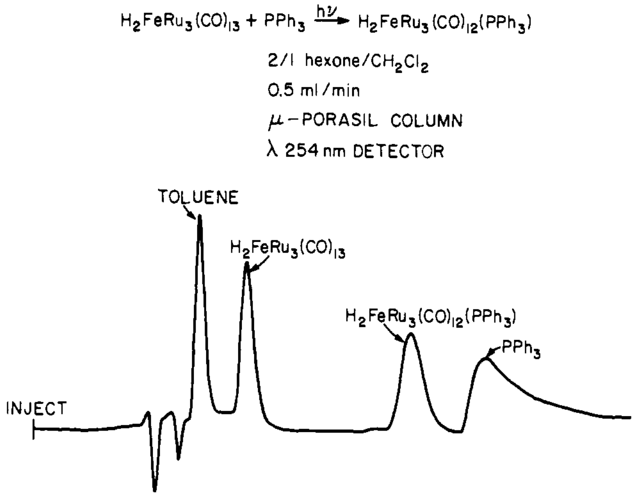

Figure 2. Liquid chromatogram obtained at an intermediate stage of photolysis during the photosubstitution of PPh_3 for CO in $H_2FeRu_3(CO)_{13}$.

The quantum yields of PPh_3 photosubstitution are set out in Table II. These yields were determined by measuring the decrease in the LC peak areas of the unsubstituted $H_2M_4(CO)_{13}$ clusters, relative to toluene as an internal standard. The values given are for conversions of less than 10% so as to minimize the effect of secondary photolysis. As indicated by the data given in Table II, the quantum yield of $H_2FeRu_3(CO)_{13}$ photosubstitution is independent of PPh_3 concentration for values of $[PPh_3]/[H_2FeRu_3(CO)_{13}]$ varying from 1.0 to 10.0.

Photosubstitution of H_2 for CO. Each of the $H_2M_4(CO)_{13}$ clusters undergoes substitution of H_2 for CO when irradiated under an H_2 atmosphere to produce the corresponding $H_4M_4(CO)_{12}$ cluster, eq 2. The $H_4Ru_4(CO)_{12}$ and $H_4FeRu_3(CO)_{12}$ products were identified by comparison of their IR spectra to reported values[14] and by comparison of LC retention times to those of authentic samples. $H_4FeOs_3(CO)_{12}$ has not been previously described but was identified by its mass spectrum, which showed

$$H_2M_4(CO)_{13} + H_2 \xrightarrow{h\nu} H_4M_4(CO)_{12} + CO \qquad (2)$$

---

(19) Hatchard, C. G.; Parker, C. A., *Proc. R. Soc. London, Ser. A* **1956**, *235*, 518.

(20) Delley, B.; Manning, M. C.; Ellis, D. E.; Berkowitz, J.; Trogler, W. C. *J. Am. Chem. Soc.*, in press.

(21) Gladfelter, W. L.; Fox, J. R.; Smegal, J. A.; Wood, T. G.; Geoffroy, G. L. *Inorg. Chem.* **1981**, *20*, 3223.

(22) (a) $H_2FeOs_3(CO)_{12}(PPh_3)$: mass spectrum, *m/e* 1226 (parent ion), 1198, 1170, 1142, 1086, 1058, 1030, 1002, 974, 946, 918, 890, 862; IR, CH_2Cl_2 solution, ν_{CO} 2100 (s), 2063 (vs), 2040 (vs), 2025 (vs), 2005 (s, sh), 1971 (s), 1855 (w), 1820 cm^{-1} (m, br). (b) $H_2FeOs_3(CO)_{11}(PPh_3)_2$: IR, CH_2Cl_2 solution, ν_{CO} 2080 (s), 2034 (vs), 2020 (vs), 2011 (vs), 1960 (s, sh), 1842 (w), 1775 cm^{-1} (m, br). The mass spectrum could not be obtained due to the lack of sufficient compound volatility.

(23) (a) $H_2Ru_4(CO)_{12}(PPh_3)$: mass spectrum, *m/e* 1004 (parent ion), 976 948, 920, 892, 864, 836, 808, 780, 758, 730, 702, 674; IR, CH_2Cl_2 solution, ν_{CO} 2070 (s), 2035 (vs), 2015 (s), 1970 (m, sh), 1810 cm^{-1} (m, br). (b) $H_2Ru_4(CO)_{11}(PPh_3)_2$: mass spectrum, *m/e* 1238 (parent ion), 1210, 1182, 1157, 1129, 1098, 1070, 1042, 1014, 986, 959, 931; IR, CH_2Cl_2 solution, ν_{CO} 2080 (w), 2057 (s), 2020 (m), 2000 (s), 1990 (s, sh), 1800 (w, br), 1775 cm^{-1} (w, br).

(24) $H_2Ru_4(CO)_{13}$ is apparently more sensitive to reaction conditions than are $H_2FeRu_3(CO)_{13}$ and $H_2FeOs_3(CO)_{13}$ since mononuclear products ($Ru(CO)_3(PPh_3)_2$ and $Ru(CO)_4PPh_3$) were observed by Wrighton and co-workers to form when $H_2Ru_4(CO)_{13}$ was stirred at room temperature in the presence of excess PPh_3 (M. S. Wrighton, private communication). We have also observed such fragmentation in the presence of a *large excess* of PPh_3 but not when the $[PPh_3]/[H_2Ru_4(CO)_{13}]$ ratio is less than 5 as is the case with the experiments reported herein.

Table III. Effect of CO on the PPh_3 Photosubstitution Quantum Yields of $H_2FeRu_3(CO)_{13}$[a]

$[CO]/[PPh_3]$	ϕ_0/ϕ[b]	$[CO]/[PPh_3]$	ϕ_0/ϕ[b]
1.0	2.03	0.25	1.17
0.75	1.98	0.10	1.13
0.50	1.52	0.00	1.00

[a] $[H_2FeRu_3(CO)_{13}] = 3.65 \times 10^{-4}$ M; $[PPh_3] = 3.65 \times 10^{-3}$ M.
[b] $\phi_0 = 2.95 \times 10^{-2}$.

a parent ion at *m/e* 966 and ions due to loss of 12 carbonyls.

The $H_2Ru_4(CO)_{13} \rightarrow H_4Ru_4(CO)_{12}$ conversion proceeds smoothly with no evidence of further reaction, but both $H_4FeRu_3(CO)_{12}$ and $H_4FeOs_3(CO)_{12}$ are photosensitive in the presence of H_2. $H_4FeRu_3(CO)_{12}$ is also thermally unstable and has been shown to decompose to yield $H_4Ru_4(CO)_{12}$ and other unidentified products.[14] This decomposition reaction is greatly photoaccelerated in the presence of H_2. $H_4FeOs_3(CO)_{12}$ is even less stable and rapidly undergoes photolysis to give a complex mixture of unidentified compounds. The 366 nm disappearance quantum yield of $H_2FeRu_3(CO)_{13}$ under H_2 is 0.015.

Photoinduced Fragmentation with CO. It has been previously shown that both $H_2FeRu_3(CO)_{13}$ and $H_2Ru_4(CO)_{13}$ thermally fragment when placed under a CO atmosphere, eq 3 and 4.[25] As

$$H_2FeRu_3(CO)_{13} + 4CO \xrightarrow[10\%\ \text{conversion}]{50\ °C,\ 42\ h} Fe(CO)_5 + Ru_3(CO)_{12} + H_2 \quad (3)$$

$$H_2Ru_4(CO)_{13} + 4CO \xrightarrow[20\%\ \text{conversion}]{25\ °C,\ 1\ h} Ru(CO)_5 + Ru_3(CO)_{12} + H_2 \quad (4)$$

the data given in eq 3 indicate, the reaction of $H_2FeRu_3(CO)_{13}$ with CO is quite slow. This reaction can be photoassisted but it is still remarkably inefficient. With use of broad-band ($\lambda \geq$ 300 nm) irradiation from a 450 W medium pressure Hg discharge lamp, photolysis of $\sim 10^{-3}$ M hydrocarbon solutions of $H_2FeRu_3(CO)_{13}$ at 25 °C under 1 atm of CO gives ~70% conversion after 43 h to $Ru_3(CO)_{12}$ and an $Fe(CO)_5/Ru(CO)_5$ mixture. Control experiments showed that little or no thermal fragmentation occurs under these conditions. For comparison, with use of this broadband irradiation, PPh_3 substitution in $H_2FeRu_3(CO)_{13}$ is ~60% complete in less than 2 h. Attempts to measure the quantum yield for the photoinduced fragmentation proved futile since the photoreaction using the less intense but monochromatic 366 nm light source is as slow as the competing thermal reaction. However, we can estimate an upper limit of $\sim 10^{-5}$ for the 366 nm quantum yield on the basis of the sensitivity of our apparatus. Similar results were obtained for $H_2Ru_4(CO)_{13}$ and $H_2FeOs_3(CO)_{13}$, although in these cases the competing thermal reactions are much more rapid.

Inhibition of PPh_3 Photosubstitution in $H_2FeRu_3(CO)_{13}$ by CO. The results presented above show that PPh_3 photosubstitution in $H_2FeRu_3(CO)_{13}$ is moderately efficient but that photoinduced fragmentation in the presence of CO does not readily occur. However, the presence of CO does have a marked inhibition effect on the PPh_3 photosubstitution quantum yield. Disappearance quantum yields of $H_2FeRu_3(CO)_{13}$ with various $[CO]/[PPh_3]$ ratios are set out in Table III. The concentration of PPh_3 was held constant in all experiments as the CO partial pressure was varied. By assuming that photolysis of $H_2FeRu_3(CO)_{13}$ induces loss of CO, eq 5, and that PPh_3 and CO compete for the photogenerated $H_2FeRu_3(CO)_{12}$ intermediate, eq 6 and 7, and by applying the steady-state approximation for $[H_2FeRu_3(CO)_{12}]$, eq 8 can be derived.[26]

$$H_2FeRu_3(CO)_{13} \xrightarrow{h\nu} H_2FeRu_3(CO)_{12} + CO \quad (5)$$

$$H_2FeRu_3(CO)_{12} + CO \xrightarrow{k_1} H_2FeRu_3(CO)_{13} \quad (6)$$

$$H_2FeRu_3(CO)_{12} + PPh_3 \xrightarrow{k_2} H_2FeRu_3(CO)_{12}(PPh_3) \quad (7)$$

Here ϕ is the quantum yield measured for

$$\frac{\phi_0}{\phi} = 1 + \frac{k_1}{k_2}\frac{[CO]}{[PPh_3]} \quad (8)$$

a given $[CO]/[PPh_3]$ ratio and ϕ_0 is the inherent quantum yield for PPh_3 photosubstitution in the absence of CO. The experimental data fit this equation quite well as indicated by the plot ϕ_0/ϕ vs. $[CO]/[PPh_3]$ shown in Figure 3. Linear least-squares analysis gives a slope of 1.06 ± 0.14 and an intercept of 0.99 ± 0.09 at 95% confidence levels. That the effect of CO is due to competition of CO with PPh_3 for a photogenerated intermediate, eq 6 and 7, and *not* to photosubstitution of CO for PPh_3 in previously formed $H_2FeRu_3(CO)_{12}(PPh_3)$ was shown by the appropriate control experiments. Photolysis of $H_2FeRu_3(CO)_{12}(PPh_3)$ under 1 atm of CO pressure gave no detectable regeneration of $H_2FeRu_3(CO)_{13}$.

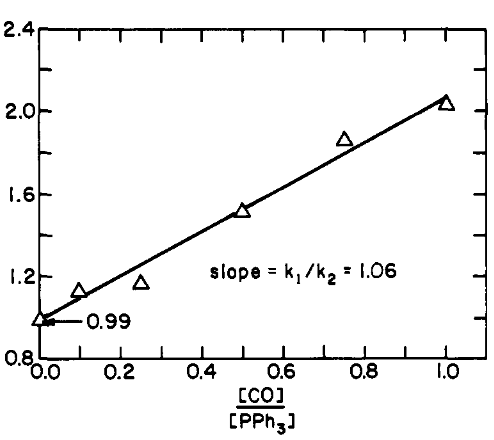

Figure 3. Graph of ϕ_0/ϕ vs. $[CO]/[PPh_3]$ for disappearance of $H_2FeRu_3(CO)_{13}$, using 366 nm irradiation in *n*-heptane solution.

Discussion

The results reported herein demonstrate that photolysis of $H_2FeRu_3(CO)_{13}$, $H_2Ru_4(CO)_{13}$, and $H_2FeOs_3(CO)_{13}$ in the presence of PPh_3 and H_2 gives photosubstitution of these ligands for CO with moderate efficiency. Although no cluster fragmentation occurs under these conditions, photolysis in the presence of CO does lead to cluster breakdown but with very low quantum efficiency. For PPh_3 photosubstitution, the mechanism outlined in eq 5–7 for $H_2FeRu_3(CO)_{13}$ appears most reasonable. This mechanism implies photoinduced CO dissociation in the primary photochemical event. The observed CO inhibition of the PPh_3 quantum yield is fully consistent with such a mechanism as indicated by the data shown in Table III and Figure 3. The k_1/k_2 ratio of 1.06 for the reactions shown in eq 6 and 7 implies that the coordinatively unsaturated $H_2FeRu_3(CO)_{12}$ intermediate has little preference for scavenging by PPh_3 or CO. This ratio is not too different from an analogous ratio of 1.36 obtained by Poë and co-workers[27] for competition between CO and PPh_3 for coordinatively unsaturated $Ru(CO)_4$, generated thermally from $Ru(CO)_5$, and is consistent with the observed substitution of PPh_3 on Ru atoms in both $H_2FeRu_3(CO)_{12}(PPh_3)$ and $H_2FeRu_3(CO)_{11}(PPh_3)_2$.[17,21]

An alternative explanation for the observed photochemistry of these tetranuclear clusters would invoke cleavage of a metal–metal bond in the primary photochemical reaction, to give a "butterfly" cluster intermediate such as **4**, eq 9. In order to satisfactorily

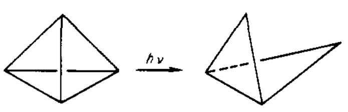

4 (9)

---

(25) Fox, J. R.; Gladfelter, W. L.; Geoffroy, G. L. *Inorg. Chem.* **1980**, *19*, 2574.

(26) The complete derivation is included in the supplementary material.

(27) Poë, A.; Chawla, S. *Inorg. Chim. Acta* **1980**, *38*, 121.

fit the kinetic data obtained for the CO inhibition of PPh_3 photosubstitution, this intermediate would have to either dissociate CO, an unlikely event for a cluster that is already electron deficient, or competively add CO or PPh_3 to give open $H_2FeRu_3(CO)_{13}L$ clusters, eq 10 and 11. Unimolecular decay of **5** and

$$4 + CO \xrightarrow{k_3} \underset{\mathbf{5}}{H_2FeRu_3(CO)_{14}} \qquad (10)$$

$$4 + PPh_3 \xrightarrow{k_5} \underset{\mathbf{6}}{H_2FeRu_3(CO)_{13}(PPh_3)} \qquad (11)$$

6 via CO loss would give $H_2FeRu_3(CO)_{13}$ and $H_2FeRu_3(CO)_{12}(PPh_3)$, respectively, but the net result would be competition of CO with PPh_3 for a common intermediate, and eq 8 would apply. Thus, the kinetic data cannot distinguish between CO dissociation or metal–metal bond cleavage in the primary photochemical event.

However, the lack of significant fragmentation of $H_2FeRu_3(CO)_{13}$ in the presence of CO does argue against metal–metal bond cleavage. An intermediate such as $H_2FeRu_3(CO)_{14}$ formed via reaction 10 is precisely the intermediate whose formation has been implicated in the rate-determining step in the thermal fragmentation of $H_2FeRu_3(CO)_{13}$ with CO.[25] However, this intermediate must decay to fragmentation products very rapidly, since it has never been detected in the thermal reactions. Thus, if this species were formed in the photochemical process, it should decay to fragmentation products and not back to $H_2FeRu_3(CO)_{13}$. Such fragmentation products were not observed and thus metal–metal bond cleavage is not implicated as the *dominant* photoreaction. Also arguing against metal–metal bond cleavage is the lack of PPh_3 concentration dependence on the quantum yield of PPh_3 photosubstitution. If photolysis were to induce metal–metal bond rupture to give an open "butterfly" cluster such as **4** in eq 9, this latter species could decay either by closure to reform the original $H_2FeRu_3(CO)_{13}$ cluster or add PPh_3 followed by CO loss to affect substitution. The relative efficiency of the latter reaction, and hence its quantum yield, would be expected to increase with increasing PPh_3 concentration. Such was not observed, Table II, and metal–metal bond cleavage as the dominant primary photoreaction is not supported. Metal–metal bond cleavage must occur some fraction of the time, however, since it is the only means by which the low quantum yield CO-induced fragmentation of the $H_4M_4(CO)_{13}$ clusters can occur.

Acknowledgment. G.L.G. gratefully acknowledges the Camille and Henry Dreyfus Foundation for a Teacher-Scholar Award (1978–1983). This research was supported by the National Science Foundation (CHE-7728387) and by the Standard Oil Company of Ohio.

Supplementary Material Available: A complete derivation of eq 8 (3 pages). Ordering information is given on any current masthead page.

Photochemistry of Surface-Confined Organometallics. Photochemical Release of a Surface-Confined Cobalt Carbonyl Catalyst[†]

Carol L. Reichel and Mark S. Wrighton*

Contribution from the Department of Chemistry, Massachusetts Institute of Technology, Cambridge, Massachusetts 02139.

Received February 9, 1981.
Revised Manuscript Received June 1, 1981

Abstract: Inorganic oxide surfaces, SiO_2 and Al_2O_3, bearing –OH functionality have been functionalized with $-Co(CO)_4$ by first treating the solids with $(EtO)_3SiH$, Me_2ClSiH, or Cl_3SiH to introduce $[S]{>}SiH$ functionality followed by reaction with $Co_2(CO)_8$. Derivatized surfaces have been characterized by infrared spectroscopy and compared to solution analogues to confirm the presence of $[S]{>}SiH$ and $[S]{>}SiCo(CO)_4$ groups on the surface. The surface-confined $[S]{>}SiCo(CO)_4$ undergoes photoreactions that begin with loss of CO subsequent to optical excitation in the near-ultraviolet. The photochemistry closely parallels the behavior of solution $R_3SiCo(CO)_4$ analogoues; CO can be photosubstituted by $P(OPh)_3$ and the surface-confined $[S]{>}SiCo(CO)_3(P(OPh)_3)$ species is detectable by infrared spectroscopy. Irradiation of the oxide powders bearing $[S]{>}SiCo(CO)_4$ suspended in Et_3SiH solutions results in the release of the $-Co(CO)_4$ into solution as $Et_3SiCo(CO)_4$ concurrent with the regeneration of surface $[S]{>}SiH$ functionality. Irradiation of the powders ($[S]{>}SiCo(CO)_4$) in the presence of 1-pentene yields $Co_4(CO)_{12}$ in solution and surface $[S]{>}Si$(pentenyl) groups. In the presence of Et_3SiH/1-pentene photoactivated catalysis by the derivatized powders ($[S]{>}SiCo(CO)_4$) occurs to give isomerization of the alkene, hydrosilation to give Et_3Si(*n*-pentyl), and small amounts of pentane. Reaction under H_2 improves the relative yield of pentane, while H_2/CO mixtures yield no hydroformylation products and lower the observed rate due to CO competing for the coordinatively unsaturated species. The surface $[S]{>}SiH$ groups also add to 1-pentene to give powders bearing $[S]{>}Si$(*n*-pentyl) functionality. The use of powders functionalized with $[S]{>}SiCo(CO)_3(P(OPh)_3)$ also gives catalysis upon photoexcitation, but the product distribution differs significantly and includes at least two isomers of Et_3Si(pentenyl). In all cases the bulk of the catalysis appears to result from Co–carbonyl fragments photoreleased from the oxide support. The initial rate of catalysis appears to depend on the initial rate at which the fragments are released into homogeneous solution. The heterogeneous photocatalysts thus give the same product distribution as appropriate homogeneous precursors, but the oxide supported $[S]{>}SiCo(CO)_4$ is more easily isolated and handled and more durable than $R_3SiCo(CO)_4$.

Chemistry of surfaces modified with molecular reagents may have use in stoichiometric and catalytic syntheses, in adhesion and other surface physical tailoring, in analysis and separations, and in chemical energy conversion.[1-10] Successful application of molecular modification depends on characterization of both the structure and reactivity of the surface-confined species. One aim of research in this laboratory has been to initiate catalysis by optical excitation of thermally inert, surface-confined or-

---

[†] Dedicated to George S. Hammond on the occasion of his 60th birthday.

(1) Murray, R. W. *Acc. Chem. Res.* **1980**, *13*, 135.
(2) Karger, B. L.; Giese, R. W. *Anal. Chem.* **1978**, *50*, 1048A.
(3) (a) Arkles, B. *CHEMTECH* **1977**, *7*, 766. (b) Whitehurst, D. D. *Ibid.* **1980**, *10*, 44.
(4) Bailey, D. C.; Langer, S. H. *Chem. Rev.* **1981**, *81*, 109.

0002-7863/81/1503-7180$01.25/0 © 1981 American Chemical Society